Corrosion Science 52 (2010) 2155–2163

Contents lists available at ScienceDirect

Corrosion Science

journal homepage: www.elsevier.com/locate/corsci

The effect of atmospheric corona treatment on AA1050 aluminium

M. Jariyaboon [a,1], P. Møller [a], R.E. Dunin-Borkowski [b], S.-I. In [c], I. Chorkendorff [c], R. Ambat [a,*]

[a] Division of Materials Science and Engineering, Department of Mechanical Engineering, Technical University of Denmark, 2800 Kgs. Lyngby, Denmark
[b] Center for Electron Nanoscopy, Technical University of Denmark, 2800 Kgs. Lyngby, Denmark
[c] Center for Individual Nanoparticle Functionality, Department of Physics, Technical University of Denmark, 2800 Kgs. Lyngby, Denmark

ARTICLE INFO

Article history:
Received 23 November 2009
Accepted 21 January 2010
Available online 1 February 2010

Keywords:
A. Aluminium
B. Polarization
C. Oxide coatings

ABSTRACT

The effect of atmospheric corona discharge on AA1050 aluminium surface was investigated using electrochemical polarization, SEM-EDX, FIB-SEM, and XPS. The corona treatment was performed with varying time (1, 5, and 15 min) in atmospheric air. A 200 nm oxide layer was generated on AA1050 after the 15 min air corona treatment. A significant reduction in anodic and cathodic reactivities was observed starting from 1 min exposure, which further decreased with prolonged exposure (15 min) and after delayed testing (after 30 days). The reduction in surface reactivity is due to the formation of thicker and denser oxide film.

1. Introduction

Use of aluminium and its alloys is extensively growing in the transportation and other technological sectors due to its light weight to reduce energy consumption and increase efficiency. In general, a pre-treatment process is used for aluminium and its alloys in order to improve paint adhesion and corrosion properties. The most common pre-treatment process presently used is chromate conversion coating, although alternatives are sought due to the toxicity of chromium ions [1]. Thus, there has been an increase in research interest to explore the feasibility of using environmentally-friendly and dry pre-treatment methods for aluminium alloys as an alternative for chrome conversion coatings.

An atmospheric corona discharge (atmospheric plasma) process, which is non-toxic, dry, easy to handle, and relatively cheap, has shown a great potential to modify the surface properties of materials such as wettability, surface energy, and adhesion [2]. It is a pre-activation technique generally applied on polymers [3–5] and papers [6] but also for aluminium foils [7] to enhance adhesion property. Brusciotti et al. [8] and Boscher et al. [9] have reported the use of atmospheric corona plasma to deposit organosilicon thin films on aluminium substrates in order to enhance the adhesion and corrosion resistance. However, they focused only on the property of thin films after atmospheric plasma deposition and the exact effect of the atmospheric corona plasma on aluminium has not yet been investigated.

Our previous study [10] has shown that the atmospheric corona discharge results in the formation of a thin oxide layer on aluminium alloy surfaces similar to conversion coatings. A significant reduction of anodic and cathodic reactivity has been observed due to oxide formation during corona treatment. The thickness of oxide layer was found to be around 150–300 nm after 20 min of the treatment.

However, the corona equipment used in our previous work was flat-bed type using substrate as one of the electrodes to generate the discharge, and therefore the clearance between electrodes was very narrow (≈1–3 mm). This was particularly a problem if the treated substrate is not fully flat, which could lead to electrical short between electrodes. Overheating of the samples and electrode was also a problem, although the plasma energy levels obtained by this equipment is high due to the small distance between the electrodes.

A more commercial friendly approach was attempted in this work to use a corona discharge torch, which blows corona produced between two electrodes onto the substrate surface. The energy level of corona discharge torch is less compared to the equipment used in our previous work. In addition, this corona torch can easily be used to treat complex surfaces or three dimensional pieces. Nowadays, the use of corona torch type as the surface pre-treatment method is extensively growing in several applications [4,5,7]. Therefore, the work presented in this paper describes a detailed investigation of the effect of corona torch discharge on

* Corresponding author. Tel.: +45 4525 2181; fax: +45 4593 6213.
E-mail addresses: scmjr@mahidol.ac.th (M. Jariyaboon), pm@mek.dtu.dk (P. Møller), rdb@cen.dtu.dk (R.E. Dunin-Borkowski), su-il.in@fysik.dtu.dk (S.-I. In), ibchork@fysik.dtu.dk (I. Chorkendorff), ram@mek.dtu.dk (R. Ambat).
[1] Department of Chemistry, Faculty of Science, Mahidol University, Bangkok 10400, Thailand.

0010-938X/$ - see front matter © 2010 Elsevier Ltd. All rights reserved.
doi:10.1016/j.corsci.2010.01.035

industrially pure AA1050 aluminium. The microstructure and thickness of oxide layer formed were investigated using SEM-EDX and FIB-SEM. The nature of oxide film was studied by XPS. Passivation of the surface due to oxide film formation as a function of corona treatment was investigated by measuring electrochemical reactivity of the surface using a micro-electrochemical technique. Passivation effect was also studied as a function of time after the corona treatment (delayed testing). Effect of hydration on the electrochemical behaviour of oxide films produced by corona followed by exposure to steam was also investigated.

2. Experimental

2.1. Material

The material used in this work was an industrially pure AA1050 (99.5 wt.%, supplied by Lemvigh-Müller A/S, Denmark) aluminium sheet with a thickness of 1 mm. All specimens were cut from the sheet with a dimension of 15 × 10 mm. Experiments were carried out on 1 μm diamond finished surface.

2.2. Corona treatment

The corona equipment used in this work was a torch type equipment namely Corona 3-Plus Model CP-Spot, Vetaphone A/S, Denmark. The corona system consisted of a generator, a HP-transformer, and electrodes. The torch containing the electrodes was mounted at approximately 3 cm above the specimen, and at an angle of 45°. The equipment configuration is illustrated in Fig. 1.

The corona discharge was operated at 230 V with a frequency of 50 Hz at a power of 0.5 kW. The exposure time was 1, 5, and 15 min unless indicated otherwise. Treatment was given in sequence with 2 min interval in between to avoid the overheating of the electrodes. Gases used in this work were atmospheric air and nitrogen (Aga, class 2.1A Adr). For delayed measurements, corona treated specimens were kept in a desiccator for 30 days.

2.3. Corona and steam treatment

Samples were treated with corona discharge for 5 min as described in Section 2.2 and then the corona treated samples were exposed immediately to steam generated from boiling deionized water for 10 min.

2.4. Microstructural analysis

The microstructure of AA1050 surface before and after corona treatment was investigated using SEM (JEOL 5900) linked with EDX.

The dual beam focused ion beam scanning electron microscopy (FIB-SEM, Quanta 3D, FEI) was used for cross-section milling of the corona treated surface in order to characterize the oxide layer generated after the treatment. The cross-section milling was performed at a tilting angle of 52°. A Ga ion beam was operated at 30 kV with a current in the range of 0.5–20 nA. Prior to milling, the area of interest was deposited by Pt with a thickness of 1 μm to avoid the damage on the surface during milling.

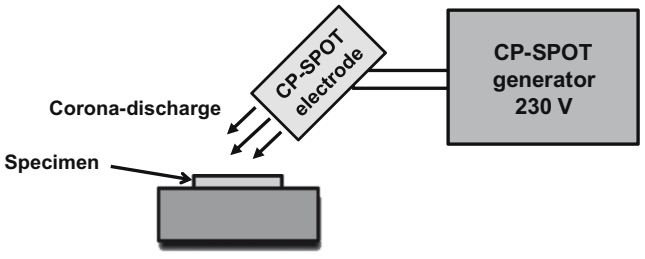

Fig. 1. Schematic of the corona equipment configuration.

2.5. XPS analysis

XPS measurements were carried out using a PHI Model 550/590 instrument operated at a pressure of 3×10^{-10} Torr. All samples were analyzed using a non-monochromatic Al Kα X-ray source operated at a power of 200 W. Specimens were fixed to the sample holder using special clips. For high resolution scans pass, energy of 25 eV was used and the number of scans was set to 20. Data analysis of the XPS spectra was done using 'CasaXPS' software, version 2.3.14. The core-level spectra were curve-fitted using a linear type background. The Al 2p ad O 1s for aluminium oxide components were fitted using a Gaussian/Lorentzian mixing ratio of 70/30. All samples were measured immediately after the corona treatment.

2.6. Local electrochemical investigations

Local electrochemical measurements were carried out using a micro-electrochemical cell with a 1 mm diameter pipette tip; details of the set-up are described elsewhere [11]. Measurements were performed on the surfaces immediately after the treatment and then the activity of the specimens were measured again on the same surfaces after keeping them in a desiccator for 30 days.

Potentiodynamic polarization was measured relative to Ag/AgCl reference electrode in naturally aerated 0.1 M NaCl solution (pH ~5). The scan rate of measurements was 1 mV/s starting from a potential close to the open circuit potential (OCP). Measurement on each sample was carried out in triplicate.

3. Results

3.1. Microstructure

Fig. 2a shows a SEM image of 1 μm finished AA1050 surface before corona treatment. It can be observed that the surface is smooth and constituent intermetallic particles are clearly seen all over the surface. Micro-hardness indentation can be seen, which was used as a reference point to observe same area before and after corona treatment.

The macroscopic image of the matt and shiny regions of 15 min atmospheric air corona treated sample is illustrated in Fig. 2c.

Fig. 2b illustrates surface morphology after 30 min atmospheric air corona treatment at the same area as shown in Fig. 2a. It is evident that the morphological effect on the surface due to corona treatment is not uniform. Some regions could be seen with a "hooked up" pattern (see arrow), while other regions are smooth. This pattern distributes non-uniformly on the surface leading to the less shiny or matt appearance (consisting of more "hooked up" patterns) on some regions than others. On treated samples, the matt and shiny regions on the AA1050 surface can be distinguished by naked eyes when the treatment time is $\geqslant$15 min.

EDX analysis was performed on the same region before and after the 30 min atmospheric air corona treatment as defined in Fig. 2a and b, respectively, and the EDX result is given in Table 1. Points 1 and 3 are the EDX analysis on the constituent intermetallic particle before and after corona treatment, respectively, and it consists of mainly Fe and Si. There is no significant difference in the composition of the intermetallic particles between untreated and air corona treated samples. In addition, oxygen cannot be detected on the particle or on the smooth areas (points 2 and 4) or in the hooked up structures (point 5).

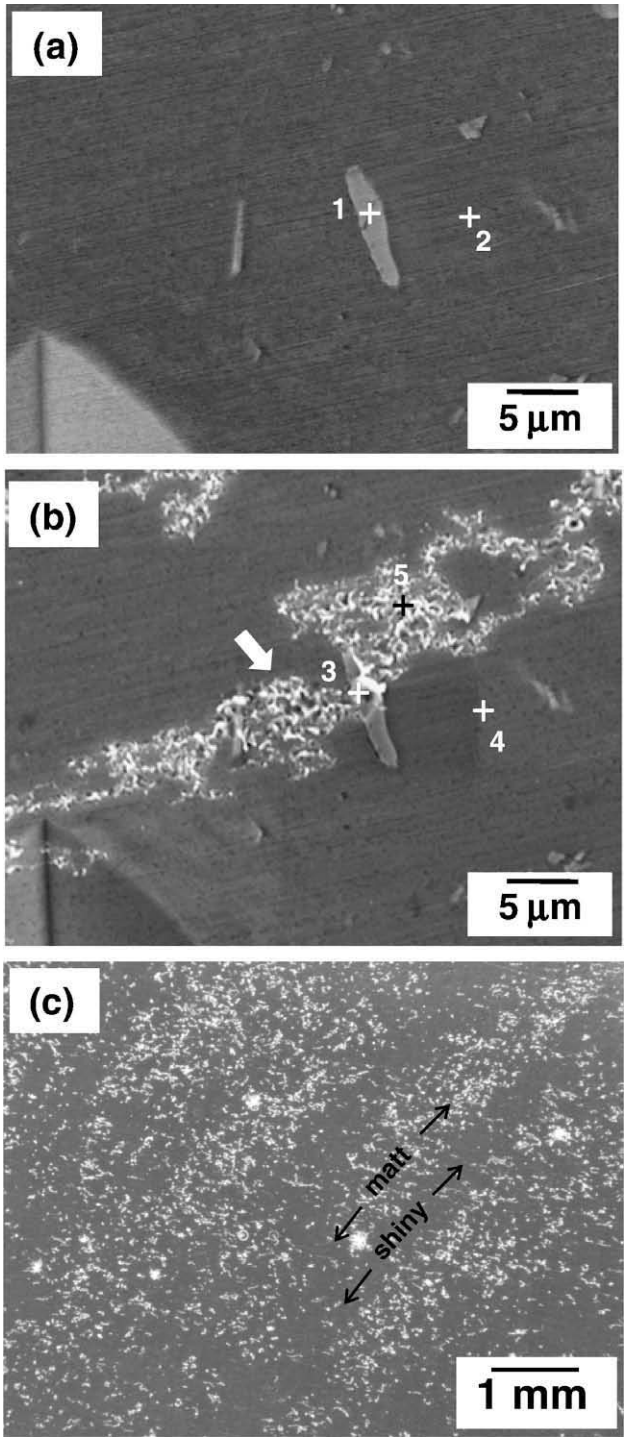

Fig. 2. (a) SEM image of 1 µm finished AA1050 surface, (b) SEM image of 30 min atmospheric air corona treated surface, and (c) optical image of 15 min atmospheric air corona treated surface. Numbers in (a) and (b) are given as references for EDX analysis.

Table 1
EDX analysis of AA1050 before and after atmospheric air corona treatment. Reference numbers are defined in Fig 2.

Detected area	Element (wt.%)			
	C	Al	Si	Fe
1. Before air corona treatment	6.00	64.89	7.44	21.67
2. Before air corona treatment	–	100	–	–
3. After air corona treatment	6.84	68.55	7.32	17.28
4. After air corona treatment	–	100	–	–
5. After air corona treatment	–	100	–	–

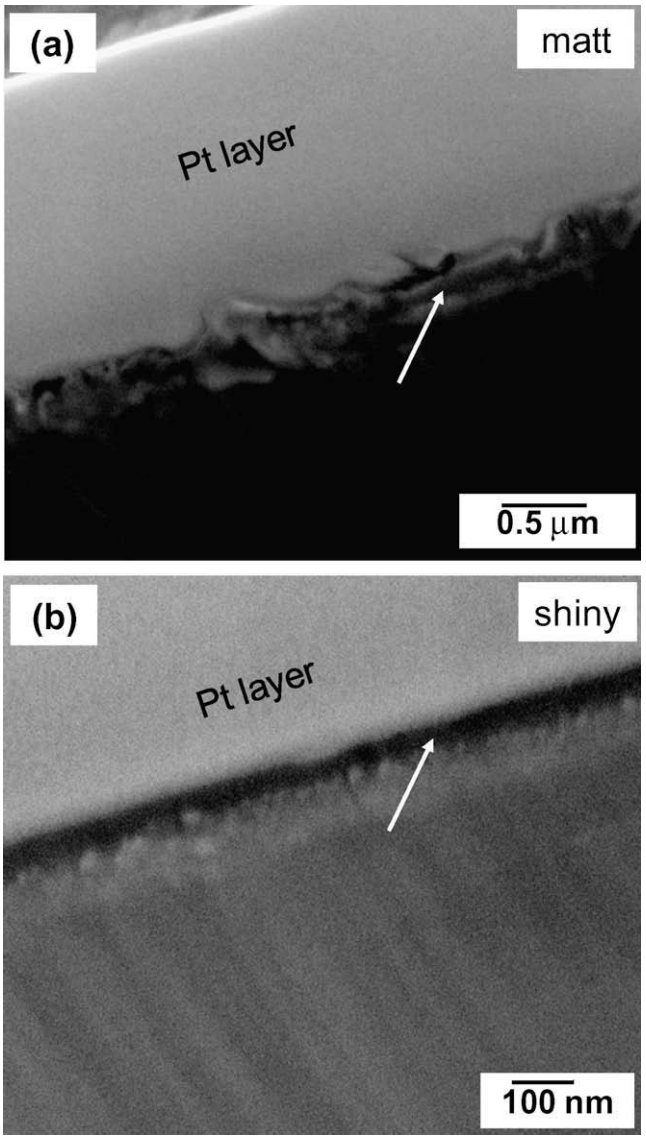

Fig. 3. FIB-SEM cross section images of a 15 min atmospheric corona treated sample: (a) matt and (b) shiny areas.

Fig. 3a and b shows the cross sectioned surfaces of AA1050 after the 15 min atmospheric air corona treatment of matt and shiny regions, respectively, using FIB-SEM. A brighter region on the top is a Pt layer which was deposited before cross-section milling to protect the area of interest from damaging during milling. Thickness of the generated oxide layer due to corona treatment of matt and shiny regions is approximately 200 and 60 nm, respectively (see arrow).

3.2. XPS analysis

As mentioned above, the surface of AA1050 after the atmospheric corona treatment appears to have two features: matt and shiny regions. XPS analysis was performed immediately on both the matt and shiny surfaces after 15 min atmospheric air corona treatment as well as on untreated surface.

XPS spectra of Al 2p peak of 15 min atmospheric air corona treated and untreated samples are illustrated in Fig. 4. In general, there

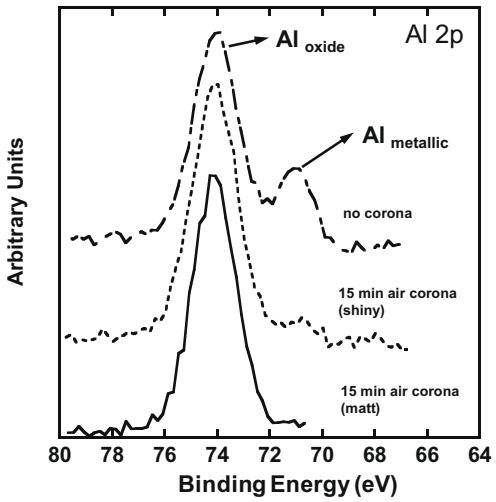

Fig. 4. Overlay plots of the Al 2p peaks of XPS analysis on the untreated surface, and shiny and matt surfaces of the 15 min atmospheric air corona treatment.

is no significant difference in binding energy position of Al 2p peak between untreated and corona treated samples. The Al 2p peak is split into two peaks which are assigned for aluminium oxide and metallic aluminium. The main peak with higher intensity and binding energy of 74.0 eV is the oxide component, and the lower intensity peak with binding energy of 71.0 eV is the metallic component.

For untreated sample, the oxide and metallic components of Al 2p peaks are distinct. After 15 min atmospheric air corona treatment, the relative intensities of oxide and metallic component peaks are changed. An increase in intensity of the oxide component peak correlated with a decrease in intensity of the metallic component peak is observed. In addition, the metallic component peak of the matt region cannot be detected, whereas for the shiny area of the same specimen, the shoulder of metallic component peak can be observed.

XPS spectra of O 1s peak of untreated and 15 min atmospheric air corona treated (matt area) samples are illustrated in Fig. 5a and b, respectively. No significant difference in the binding energy position of O 1s peak is seen between untreated and atmospheric air corona treated samples. An asymmetric peak with a shoulder at the higher binding energy can be observed. Curve fitting shows that the O 1s peak consists of two components: aluminium oxide at 530.5 eV and aluminium hydroxide at 531.8 eV. It is evident that for the untreated sample, peak areas of the hydroxide and oxide components are similar and the ratio of the peak areas of hydroxide component to oxide component is 0.93. After atmospheric air corona treatment for 15 min, an increase in the oxide component correlated with a decrease in the hydroxide component is clearly seen. The hydroxide/oxide peak area ratio is 0.35.

3.3. Local electrochemical measurements

Anodic and cathodic polarization curves were measured on untreated and treated corona surfaces using a micro-electrochemical cell with a diameter of the exposure area of 1 mm. The corona treatment conditions were 1, 5, and 15 min atmospheric air corona and 15 min nitrogen corona. Anodic and cathodic reactivities of the matt and shiny regions of the 15 min atmospheric air corona treatment were also investigated. All measurements were performed immediately after corona treatments and 30 days after the treatments to investigate delayed behaviour.

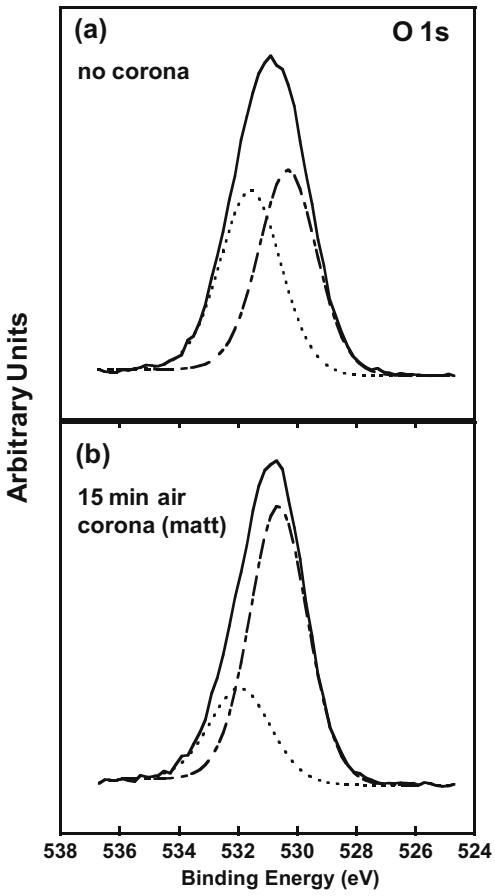

Fig. 5. XPS spectra of O 1s peak of (a) untreated and (b) 15 min atmospheric air corona treated (matt area) samples.

The effect of hydration on corona treated sample was investigated by anodic polarization measurements. Anodic polarization was measured immediately after 5 min atmospheric air corona treatment followed by 10 min steam exposure from boiling deionized water.

3.3.1. Anodic reactivity measured immediately after the corona treatment

Fig. 6a shows anodic polarization curves measured immediately after the corona treatment. In general, the corona treatment shifts the E_{corr} to more positive (noble) direction compared with untreated specimen. Overall a shift of ~300 mV is observed between fresh sample and 15 min air corona treated sample (matt region).

It is evident that an influence is already seen with a very short treatment time of 1 min atmospheric air corona treatment. The anodic reactivity at all potentials has decreased considerably (except for 1 min atmospheric corona treatment at high potential). A passive region appears when increasing the time of atmospheric air corona treatment to 5 and 15 min. The average breakdown potentials of 5 and 15 min atmospheric air corona treatment (matt region) are −516 and −294 mV, respectively. The anodic current of the 15 min atmospheric air corona treated sample is approximately 100 times less than that of the untreated sample.

The 15 min nitrogen corona treatment seems to have less influence compared with the 15 min atmospheric air corona treatment. However, still a large reduction of E_{corr} and anodic current associated with the presence of a passive region can clearly be seen.

Comparison between matt and shiny surfaces of the 15 min atmospheric air corona treatment shows that the matt surface

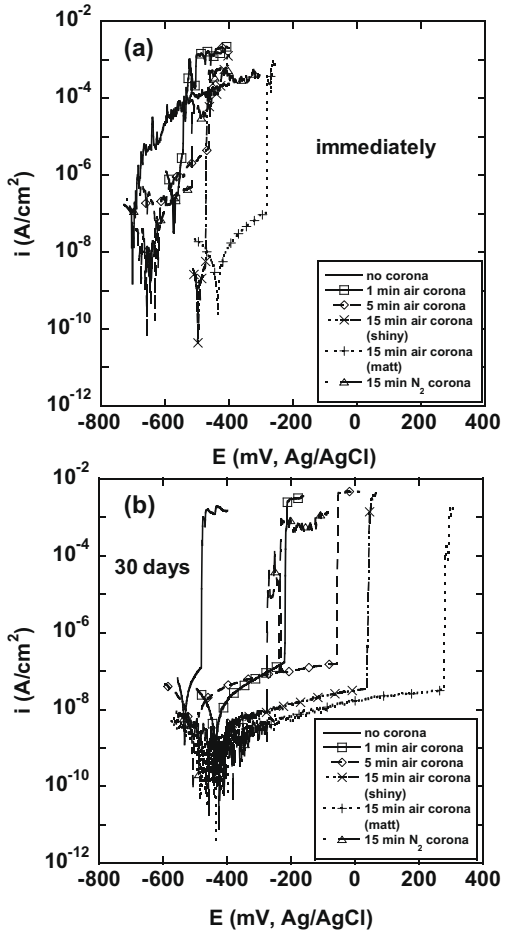

Fig. 6. Anodic polarization curves of untreated and corona treated specimens measured (a) immediately and (b) 30 days after the treatments. All measurements were performed using a micro-electrochemical cell.

has lower anodic reactivity. This result is in good agreement with XPS analysis and FIB-SEM images showing the thicker oxide layer in the matt area.

3.3.2. Anodic reactivity measured 30 days after the corona treatment

Fig. 6b reveals anodic polarization curves measured 30 days after introducing the corona treatment. A significant improvement in corrosion resistance is clearly seen for all treatments comparing the curves immediately after the treatments shown in Fig. 6a. Curves for corona treated samples exhibit a long passive region with approximately 10 times lower anodic current and much higher breakdown potentials compared with anodic polarization curves measured immediately after the corona treatments.

3.3.3. Anodic reactivity measured immediately after the corona and steam treatment

Fig. 7 shows anodic polarization curves measured for 5 min air corona followed by 10 min steam treated sample in comparison with 10 min steam treated sample, 5 min air corona treated samples measured immediately, and 30 days after introducing corona treatment. It is evident that the 5 min air corona followed by 10 min steam treated sample shows lower anodic reactivity compared with 10 min steam treatment and 5 min air corona treatment measured immediately (lower anodic current and larger passive region). Furthermore, the 5 min air corona followed by 10 min steam treated sample shows similar anodic current and

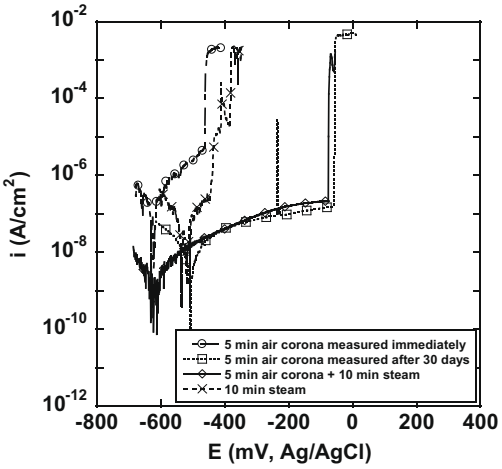

Fig. 7. Anodic polarization curves of 5 min atmospheric air corona treated specimens measured immediately and 30 days after the treatment, 5 min atmospheric air corona followed by 10 min steam treated specimen, and 10 min steam treated specimen.

breakdown potential to that of the 5 min corona treated sample measured 30 days after introducing the corona treatment.

To compare the anodic reactivity of all conditions, a summary of average values of anodic over potentials at 10^{-6} A/cm^2 is plotted as presented in Fig. 8. It is evident that an increase in time of atmospheric air corona treatment increases the anodic over potentials during polarization experiments. After 30 days, the anodic over potentials have dramatically increased compared to the immediate measurements in the range of 330–560 mV (Ag/AgCl) depending on the treatment time. The highest increment is for the 15 min atmospheric air corona treated sample. The 5 min air corona followed by 10 min steam treated sample shows higher anodic over potentials than that of the untreated, 1, 5, 15 min air corona treated and 15 min N_2 corona treated samples measured immediately after the treatment, while it shows comparable anodic over potentials to that of the 5 and 15 min (shiny region) air corona treated samples measured 30 days after the treatment.

It should be noted that the anodic over potential of 15 min nitrogen corona treated sample measured immediately after the treatment is in the same range as the 15 min atmospheric air corona treatment, but after 30 days, the anodic over potential is in the same level as the 1 min atmospheric air corona treated sample. However, the anodic current at the passive region is similar to that of the 15 min atmospheric air corona treated sample.

Fig. 9a and c illustrates examples of corrosion morphology after anodic polarization measurements of 5 and 15 min atmospheric air corona treated samples kept for 30 days, respectively. For 5 min air corona treated sample, two pits are observed, while for 15 min air corona treated sample, only one pit is seen. Pit morphology shows crystallographic dissolution and the un-dissolved crystallographic planes are [1 0 0]. Fig. 9b shows higher magnification SEM image of the 5 min air corona treated sample with a tilting angle of 32° within the rectangular area as indicated in Fig. 9a, and Fig. 9d shows higher magnification SEM image of 15 min air corona treated sample with a tilting angle of 40° within the rectangular area as indicated in Fig. 9c. The remains of un-dissolved thin oxide layer near the edge of pit can be seen as indicated by arrows and also oxides on the "hooked up" structure shown in Fig. 9d.

3.3.4. Cathodic reactivity measured immediately after the corona treatment

Fig. 10a illustrates cathodic polarization curves measured immediately after the corona treatments. It can be seen that the

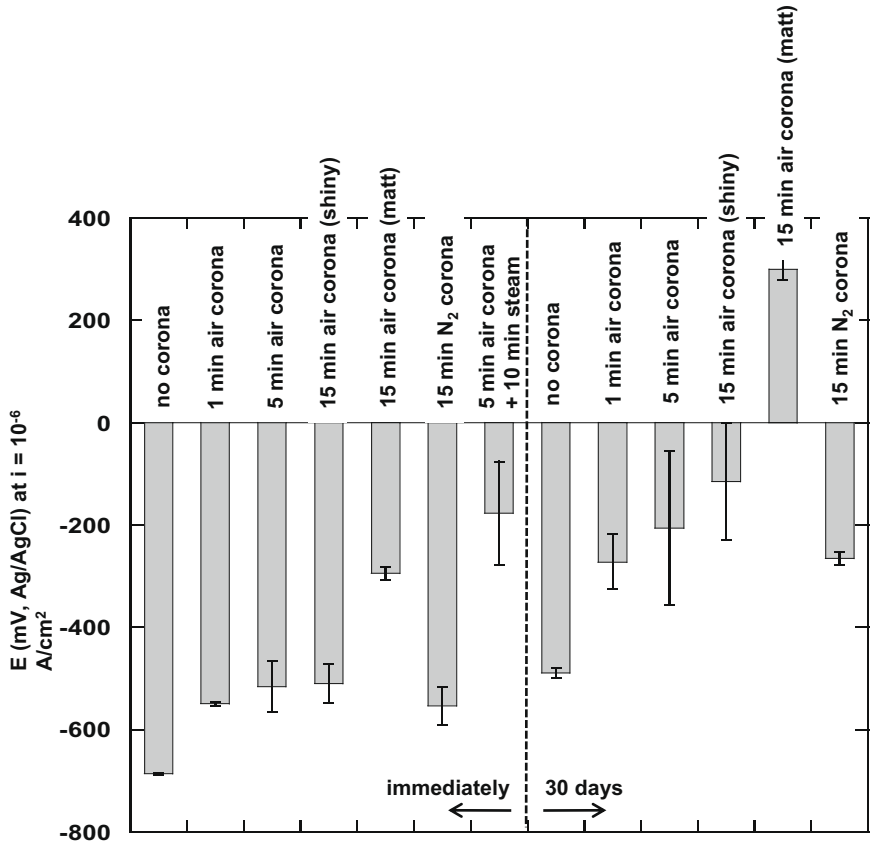

Fig. 8. Average values of anodic over potentials at 10^{-6} A/cm^2 of untreated and treated corona specimens measured immediately and 30 days after the treatments as well as 5 min air corona followed by 10 min steam treatment.

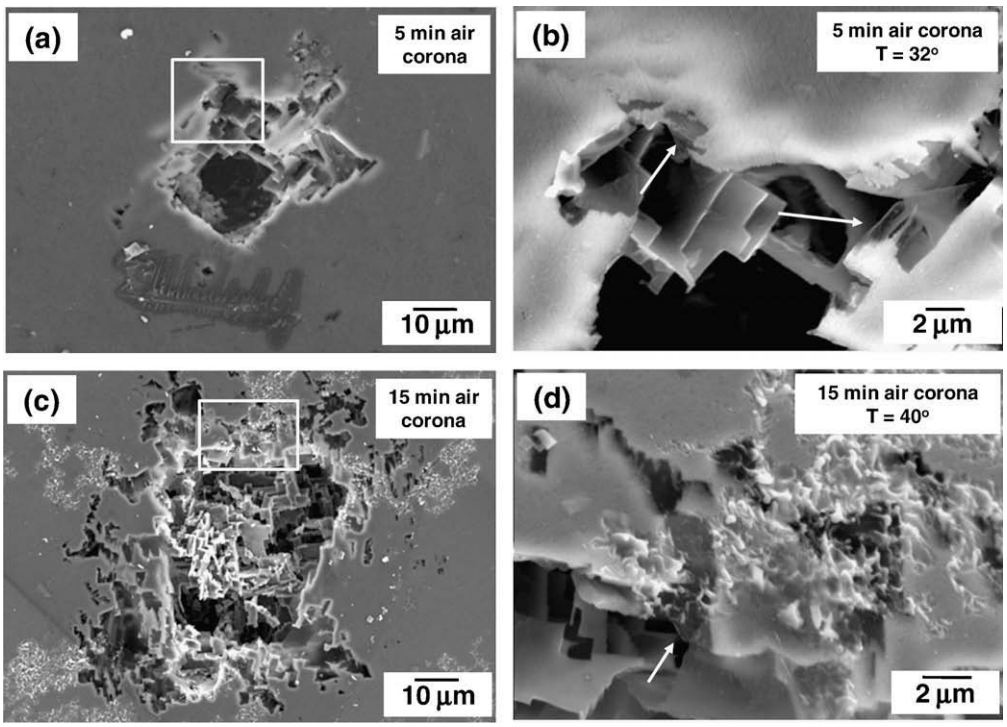

Fig. 9. SEM images showing pits after anodic polarization: (a) 5 min atmospheric air corona treated sample, (b) higher magnification of rectangular area indicated in (a) with a tilting angle of 32°, (c) 15 min atmospheric air corona treated sample, and (d) higher magnification of rectangular area indicated in (c) with a tilting angle of 40°.

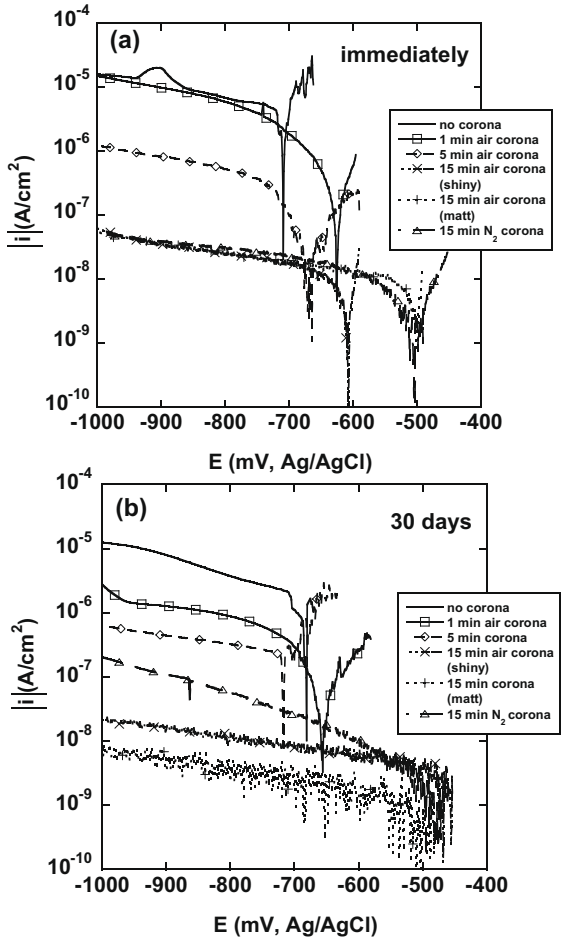

Fig. 10. Cathodic polarization curves of untreated and corona treated specimens measured (a) immediately and (b) 30 days after the treatments. All measurements were performed using a micro-electrochemical cell.

1 min atmospheric air corona treatment has no influence on the cathodic current. A reduction in cathodic current appears when increasing the treatment time to 5 min, which shows a current approximately 10 times lower than the untreated specimen. A significant reduction of cathodic current with an order of hundred times can be observed for the 15 min atmospheric air corona (both matt and shiny areas) and the 15 min nitrogen corona treatments.

3.3.5. Cathodic reactivity measured 30 days after the corona treatment

Fig. 10b shows cathodic polarization curves measured 30 days after the treatment. For all atmospheric air corona treatments, the cathodic current is reduced by half a decade compared to measurements taken immediately after corona treatment. It should be noted that the matt area of the 15 min atmospheric corona treatment shows a lower cathodic current than that of the shiny area. Surprisingly, for the 15 min nitrogen corona treatment, the cathodic current has increased by an order of a half decade compared with the immediate measurements.

The cathodic reactivity after all the treatment is summarized in Fig. 11, in which the magnitude of average value of cathodic current density at −850 mV (Ag/AgCl) is plotted. It is evident that the corona treatment can significantly reduce the cathodic reactivity. An increase in storing time after the treatment further decreases the cathodic current except for the 15 min nitrogen corona treatment.

4. Discussion

Our past work [10] showed that an oxide layer with a thickness of 150–300 nm can be generated on aluminium alloys using the specially designed flat-bed type atmospheric air corona equipment which was operated at high energy (20 kV, 20 kHz, 1 kW). Corona was generated using the substrate as one electrode and the other electrode is separated from the surface with a clearance of approximately 1–3 mm.

The work done by Boscher et al. [9] revealed that the polysiloxane thin film on aluminium foil can be produced by atmospheric plasma treatment. The film composition depends on the amount of oxygen in the plasma gas, and anodic current of aluminium foil is decreased up to ~3 orders of magnitude after the deposition of the polysiloxane film. However, the improvement of corrosion behaviour of the aluminium foil might also be due to the oxide film growth as seen in this study. It should be noted that Boscher et al. did not mention the treatment time as if the treatment is short; the effect due to the oxide film growth is less.

In this study, the inhomogeneous appearance of the corona treated surface showing the matt and shiny areas is possibly due to a difference in corona discharge energy at each region, which might lead to intermittent sparking at some locations. This discrete intense spark is originated from localized regions of the electrode [12]. Higher energy at some regions is due to the flow pattern of corona filed or sparking gives a matt surface finish with features seen in Fig. 2b and c.

It is well known that the surfaces of aluminium and its alloys exposed to the normal atmospheric air are covered with an amorphous passive oxide film with a thickness of approximately 5 nm. The inner layer is the compact oxide whereas the outer layer is the permeable hydrated oxide [1]. This native oxide film protects aluminium and its alloys from corrosion [1]. In this work, the oxide layer with a thickness of approximately 60–200 nm (over shiny and matt region) is formed after atmospheric air corona treatment for 15 min using a commercially available corona torch operated at lower energy (230 V, 50 Hz, 0.5 kW) compared with our earlier work [10].

XPS spectra of Al 2p peak of oxide film on aluminium surface contain two components: metallic component and oxide component. The oxide component of Al 2p peak consists of both aluminium oxide and aluminium hydroxide species and it is very difficult to distinguish between these two species using Al 2p peak [13]. In addition, a variation of binding energy of each oxide/hydroxide compound has been reported depending on analysis techniques as well as instrument employed [10,14].

The work done by Ocal et al. [15] showed that the separation of binding energy of Al 2p peak associated with oxidation can be varied from 2.6 to 3.7 eV depending on the several factors such as the method of oxide growth. For 'air-passivated' amorphous oxides, several authors [15–17] showed that the separation of the binding energies of Al 2p peak is in a range of 2.6–2.8 eV, but Halverson and Cocke [18] showed that the separation of the binding energy of the native oxide film is 2.93 eV. For oxides produced by plasma treatment, Strohmeier [16] and Li et al. [17] reported that the separation of the binding energy of Al 2p peak are 2.9 and 2.7 eV, respectively, whereas Halverson and Cocke [18] found the binding energy separation of 3.4–3.6 eV. They also claimed that the binding energy separation of 3.4–3.6 eV for plasma grown film is an indication of the crystallinity of the film.

As illustrated in Fig. 4, the relative intensities between oxide component and metallic component of the Al 2p peak are increased after the 15 min atmospheric corona treatment indicating an increase in the oxide film thickness. The oxide film thickness of the matt region of the 15 min air corona treatment is thicker than

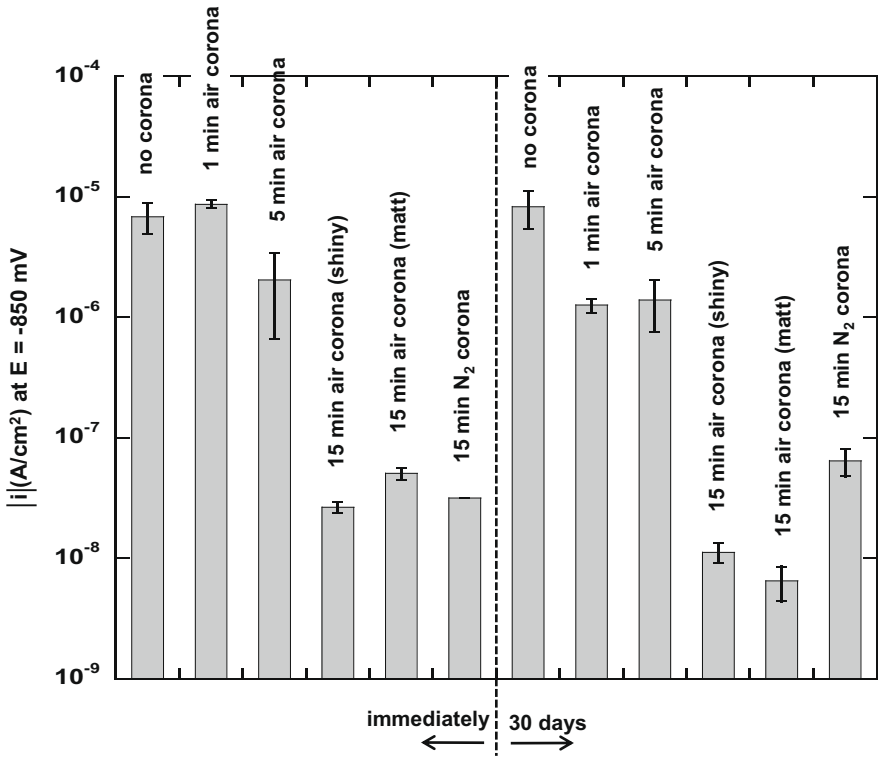

Fig. 11. Average values of cathodic current density at $E = -850$ mV (Ag/AgCl) of untreated and treated corona specimens measured immediately and 30 days after the treatment.

that of the shiny region and also thicker than the depth of XPS analysis. Although the binding energy separation of Al 2p peak seems to be useful to obtain information regarding the nature of oxide film, a large variation still exists as mentioned earlier. In this study, no concrete conclusion on the nature of oxide film can be made based on Al 2p peak.

XPS spectra of O 1s peak can give the information of the relative amount of O–H bonding in the aluminium oxide film. A higher binding energy peak is a characteristic of aluminium hydroxide and a lower binding energy peak is a characteristic of aluminium oxide [13,16,17,19]. In this work, it shows that the hydroxide/oxide peak area ratio is reduced from 0.93 to 0.35 after 15 min air atmospheric corona treatment indicating less amount of hydroxide component in the oxide film (Fig. 5). This suggests that the oxide film generated by atmospheric corona treatment is denser than the native oxide film. Li et al. [17] showed that the oxide film generated by plasma treatment initially grows linearly as a function of exposure time. It indicates that the mechanism of oxide film generated by plasma treatment is a diffusion mechanism which gives a higher density of oxide film than that of native oxide film.

4.1. Corrosion behaviour

As illustrated in Figs. 6a and 8, an increase in time of corona treatment significantly decreases anodic reactivity of AA1050. The 15 min atmospheric air corona treatment (matt area) reduces the anodic reactivity by an order of 100 times. This result is in good agreement with FIB-SEM (Fig. 3), XPS analysis (Figs. 4 and 5), and corrosion morphology (Fig. 9). Dramatic decrease in the anodic reactivity is due to the grown oxide film with corona treatment and denser oxide layer as shown by the XPS which acts as a corrosion barrier.

Cathodic reactivity shows a similar behaviour as the anodic reactivity; the cathodic reactivity decreases with an increase in time of corona treatment as shown in Fig. 10a and 11. The result is in good agreement with the morphology of Fe-containing intermetallic particles after the prolonged corona treatment. The selective oxidation of the Fe-containing intermetallic particles cannot be observed as illustrated in Fig. 2. Our past work [10] on the contrary showed that the selective oxidation of the Fe-containing intermetallic particles may cause an increase in cathodic current after the prolonged corona treatment. Fe^{3+} containing oxides are possibly produced after the selective oxidation and they are likely to be reduced during the cathodic reaction resulting in an increase in cathodic current. However, in this work, the reduction in cathodic reactivity is assumed to be due to the growth of the oxide layer all over the surface, which protects the particles participation in the cathodic reaction.

The effect caused by the atmospheric corona treatment not only remains after 30 days, but also significantly improves the corrosion resistance of specimens as illustrated in Figs. 6b, 8, 10b, and 11. This is likely to be associated with the surface hydration of the films after exposure to the moisture in the atmosphere for a long time. Although the XPS measurements of corona treated samples after introducing the treatment for 30 days did not perform, it is well known that the surface hydration of oxide film on aluminium occurs when the surface exposes to the atmosphere. In addition, it is also in good agreement with the corrosion behaviour of 5 min corona followed by 10 min steam treated sample as revealed in Figs. 7 and 8. It shows that using atmospheric air corona treatment before exposure to steam gives much lower anodic reactivity compared with treating sample only with steam. It suggests that the air atmospheric corona can create the reactive surface for surface hydration to occur leading to a reduction in reactivity.

Comparing anodic and cathodic reactivities between 15 min atmospheric air corona and 15 min N_2 corona treatments (Figs. 6, 8, 10, and 11), it is evident that N_2 corona treated samples show higher corrosion susceptibility than that of atmospheric air corona

treated specimens although the reactivity N_2 corona treated samples as well reduced significantly compared to untreated samples. It suggests that atmospheric air corona treatment is more effective due to the presence of higher amounts of oxygen than that of N_2 corona treatment for creating corrosion resistant oxide film on aluminium surface. Using atmospheric air, more oxygen plasma will be generated and high concentration of oxygen in plasma gas is a good precursor to create oxide film on aluminium surface.

In summary, the results presented in this paper suggest the feasibility of using atmospheric air corona to generate an oxide film on the aluminium alloy surface, although further investigations are needed to optimize various parameters. The thickness of the oxide layer formed in this case is similar to standard chromate conversion treatment (such as Alodine), which is approximately 125–250 nm [20].

5. Conclusions

1. This investigation has shown the potential of using a corona discharge torch operated at low energy (230 kV, 50 Hz, 0.5 kW) to produce a thin oxide layer on AA1050 aluminium surface in order to enhance corrosion resistance.
2. Using corona discharge torch, a thin oxide layer with a thickness of approximately 200 nm (matt area) and 60 nm (shiny area) has been produced on aluminium surface after 15 min atmospheric air corona treatment.
3. Due to the formation of the generated oxide layer, a significant decrease in both anodic and cathodic reactivities has been observed as a function of treatment time. The anodic and cathodic reactivities can be reduced up to approximately 100 times by 15 min atmospheric air corona treatment.
4. Prolonged exposure to atmospheric air after the corona treatment has resulted in further decrease in both anodic and cathodic reactivities. After 30 days exposure to atmospheric air after atmospheric air corona treatment for 15 min, the hydration of the formed oxide layer has reduced the anodic reactivity by ten times, while cathodic reactivity has decreased by five times.

Acknowledgements

M. Jariyaboon is supported by The Hans Christian Ørsted Postdoc Fellowship Programme. The authors thank A. Nicole MacDonald (Center for Electron Nanoscopy, Technical University of Denmark) for her assistance in FIB-SEM. CINF is funded by the Danish National Research Foundation.

References

[1] J.R. Davis, Corrosion of Aluminum and Aluminum Alloys, ASM International, OH, 1999.
[2] C. Tendero, C. Tixier, P. Tristant, J. Desmaison, P. Leprince, Atmospheric pressure plasma: a review, Spectrochim. Acta B 61 (2006) 2–30.
[3] E.T. Kang, Z.H. Ma, K.L. Tan, B.R. Zhu, Y. Uyama, Y. Ikada, Surface modification and functionalization of electroactive polymer films, Polym. Adv. Technol. 10 (1999) 421–428.
[4] R. Stewart, V. Goodship, F. Guild, M. Green, J. Farrow, Investigation and demonstration of the durability of air plasma pre-treatment on polypropylene automotive bumpers, Int. J. Adhes. 25 (2005) 93–99.
[5] M. Pascual, R. Balart, L. Sánchez, O. Fenollar, O. Calvo, Study of the aging process of corona discharge plasma effects on low density polyethylene film surface, J. Mater. Sci. 43 (2008) 4901–4909.
[6] M. Pykönen, H. Sundqvist, J. Järnström, O.-V. Kaukoniemi, M. Tuominen, J. Lahti, J. Peltonen, P. Fardim, M. Toivakka, Effect of atmospheric plasma activation on surface properties of pigment-coated and surface-sized paper, Appl. Surf. Sci. 255 (2008) 3217–3229.
[7] Private communication with Mr. Jan Eisby, Vetaphone A/S, Kolding, Denmark, 2006.
[8] F. Brusciotti, A. Batan, I. De Graeve, M. Wenkin, F. Reniers, J.J. Pireaux, M. Piens, J. Vereecken, H. Terryn, Characterization of hybrid organic/silicon based coatings deposited by wet and plasma deposition methods on Al substrates, in: Fifth International Symposium on Aluminium Surface Science and Technology, Leiden, The Netherlands, 2009.
[9] N.D. Boscher, P. Choquet, D. Duday, H.-N. Migeon, Atmospheric pressure dielectric barrier discharge deposition of organosilicon thin films for aluminium corrosion protection, in: Fifth International Symposium on Aluminium Surface Science and Technology, Leiden, The Netherlands, 2009.
[10] D. Minzari, P. Møller, P. Kingshott, L.H. Christensen, R. Ambat, Surface oxide formation during corona discharge treatment of AA 1050 aluminium surfaces, Corros. Sci. 50 (2008) 1321–1330.
[11] M. Jariyaboon, A.J. Davenport, R. Ambat, B.J. Connolly, S.W. Williams, D.A. Price, The effect of welding parameters on the corrosion behaviour of friction stir welded AA2024-T351, Corros. Sci. 49 (2007) 877–909.
[12] D. Briggs, Corona discharge treatment, in: D.E. Packham (Ed.), Handbook of Adhesion, John Wiley & Sons Ltd, Chichester, 2005, pp. 89–90.
[13] B.R. Strohmeier, An ESCA method for determining the oxide thickness on aluminum-alloys, Surf. Interface Anal. 15 (1990) 51–56.
[14] D. Briggs, M.P. Seah, Practical Surface Analysis Auger and X-ray Photoelectron Spectroscopy, vol. 1, second ed., John Wiley, Chichester, 1990.
[15] C. Ocal, B. Basurco, S. Ferrer, An ISS-XPS study on the oxidation of Al (1 1 1) – identification of stoichiometric and reduced oxide surfaces, Surf. Sci. 157 (1985) 233–243.
[16] B.R. Strohmeier, The effect of O_2 plasma treatments on the surface-composition and wettability of cold-rolled aluminum foil, J. Vac. Sci. Technol. A 7 (1989) 3238–3245.
[17] H. Li, A. Belkind, F. Jansen, Z. Orban, An in situ XPS study of oxygen plasma cleaning of aluminum surfaces, Surf. Coat. Technol. 92 (1997) 171–177.
[18] D.E. Halverson, D.L. Cocke, Investigation of plasma-grown planar alumina films for use in the modeling of bulk alumina, Thin Solid Films 155 (1987) 133–142.
[19] N.A. Thorne, P. Thuéry, A. Frichet, P. Gimenez, A. Sartre, Hydration of oxide-films on aluminum and its relation to polymer adhesion, Surf. Interface Anal. 16 (1990) 236–240.
[20] Technical Service Bulletin, Hankel Surface Technologies. Available from: <http://www.casa.co.nz/material/Finishing/Alodine1200LDipSpray.pdf/> (accessed 13.10.09).